

Received April 20, 2018, accepted June 2, 2018, date of publication June 6, 2018, date of current version July 6, 2018.

Digital Object Identifier 10.1109/ACCESS.2018.2844556

# Experimental Research of Multistatic Passive Radar With a Single Antenna for Drone Detection

**GAO FANG, JIANXIN YI<sup>ID</sup>, (Member, IEEE), XIANRONG WAN<sup>ID</sup>, YUQI LIU, AND HENGYU KE**

Radio Detection Research Center, School of Electronic Information, Wuhan University, Wuhan 430072, China

Corresponding author: Jianxin Yi (jxyi@whu.edu.cn)

This work was supported in part by the National Key Research and Development Plan of China under Grant 2016YFB0502403, in part by the Postdoctoral Innovation Talent Support Program under Grant BX201600117, in part by the National Natural Science Foundation of China under Grant 61701350 and Grant 61331012, and in part by the Support Program of Hubei Province under Grant 2015BCE075 and Grant 2016CFA061.

**ABSTRACT** Digital television signals are attractive illuminations of opportunity for the passive radars in the field of low altitude and slow speed target detection. The digital television standard permits reconstruction of a reference signal using the received signal in surveillance channel, which enables a single-antenna digital television based passive radar (SDPR) processing. This paper investigates the practical feasibility of a multistatic SDPR (MSDPR) for the drone detection. First, the detection range of the SDPR is analyzed in terms of signal processing procedures involving multipath energy, extracted reference signal purity, and receiving antenna. Second, according to the characteristics of the SDPR, the reference signal extraction is analyzed. In addition, considering that the SDPR cannot locate and track the detected target, a novel MSDPR processing method is proposed. The core idea of this method is to use the optimal reference signal extracted from the receiving station with the least interference as the shared reference signal in MSDPR, which can greatly improve the system detection capability. Finally, the small drone detection experiments using the MSDPR are presented. The theoretical considerations are demonstrated using the experimental data.

**INDEX TERMS** Passive radar with a single antenna, multistatic passive radar, drone detection and tracking, digital television signal.

## I. INTRODUCTION

In recent years, the use of micro-Unmanned Air Vehicles (UAVs) or drones has risen exponentially due to their low costs and simple operations. These platforms can be used for private leisure and filming, and also for applications such as disaster response, search and rescue, and agricultural/environment monitoring. However, there are many potential misuses involving drones, such as violation of privacy, smuggling, espionage or even disrupting flights, which may pose serious threats on public safety and air traffic [1]. Thus, drone detection, tracking and interception system gradually become hot topics. The typical features of the drones are Low altitude, Small radar cross-section (RCS), and Slow speed (LSS). It poses great challenges for radar detection especially in urban area.

Digital television broadcasting (digital video broadcasting–terrestrial (DVB-T), Digital Television Terrestrial Multimedia Broadcasting (DTMB), and China mobile multimedia broadcasting (CMMB)) signals with orthogonal frequency

division multiplex (OFDM) modulation are the most widely used illuminations of opportunity for passive radars [2]–[6]. The high radiated power and omnidirectional low altitude coverage of these signals make them easy for the detection of the small-RCS, and low-altitude targets. In addition, continuous emission and wide bandwidth of these signals make them possible to continuously detect slow-speed and small targets. Therefore, it is feasible to utilize the digital television broadcasting signals as illumination sources to detect the UAVs [7], [8].

The conventional architecture of passive radar (PR) consists of two channels: a reference channel for the reception of the direct-path signal and a surveillance channel for the reception of the target echoes [9]–[12]. In practice, the surveillance channel also inevitably collects reflections from the static scatterers (static clutter), and a direct-path signal. The direct-path signal (or static clutter) is usually dominant in the surveillance channel [3], [13]. Moreover, the dominant direct-path signal (or the strongest static clutter) in the

reference channel is considered as an effective signal [14]–[18]. This makes it possible to recover the reference signal by reconstructing the surveillance signal [19]. Therefore, a new idea is proposed to utilize a compact single-antenna receiver for the UAV detection.

Differing from the typical PR, the single-antenna digital television based passive radar (SDPR) has only a single receiver channel which is used as the reference and surveillance channel simultaneously. For the reference channel, it is desirable to have a high direct-path signal to interference plus noise ratio (SINR). In contrast, for the surveillance channel, it is desirable to avoid strong direct-path (multipath) interference and receive the target echoes. For the passive radar with a single receiver channel, it is obvious that a high direct-path SINR is beneficial to extract the pure reference signal. But the strong direct-path signal would mask the target echoes and occupy the dynamic range of the receiver channel, which severely degrades the detection performance. Thus, it is worthy to consider how to reasonably configure the direct-path signal energy so that the detection performance is maximized.

The SDPR has been first studied by [19]–[22]. Reference [19] showed that the reference signal was recovered by remodulation of the surveillance channel. Reference [20] illustrated that a passive radar with a single channel is possible using distant transmitters, with a reference signal to noise ratio (SNR) close to 0 dB. Reference [21] used specifically OFDM signals to detect a target through delay-Doppler processing. Reference [22] proposed a processing scheme including reference signal reconstruction and static clutter suppression, and used Monte-Carlo simulations to quantitatively evaluate the performance against different direct-path SNR values. At last, they presented the real-data results to validate the feasibility of the SDPR. Nevertheless, theoretical analysis of the detection performance was inadequate and comparative experiments with the typical PR were not reported. Besides, target locating and tracking using multistatic SDPR (MSDPR) has not been considered.

To give insights into the SDPR, this paper tries to analyze the detection range in terms of signal processing procedures involving multipath energy, extracted reference signal purity, and receiving antenna. According to the characteristics of the SDPR, the reference signal extraction is analyzed. As there is no way for a SDPR to locate and track the detected targets, a novel MSDPR processing method is proposed. The core idea of this method is to use the optimal reference signal extracted from the receiving station with the least interference as the shared reference signal in MSDPR, which can resist strong interference, reduce computational burden, and also greatly improves system detection capability. Furthermore, the effectiveness of the proposed methods is verified by field experiments.

This paper is organized as follows. The SDPR detection performance is analyzed in Section II. The signal processing methods including the reference signal extraction and MSDPR signal processing are proposed in Section III.

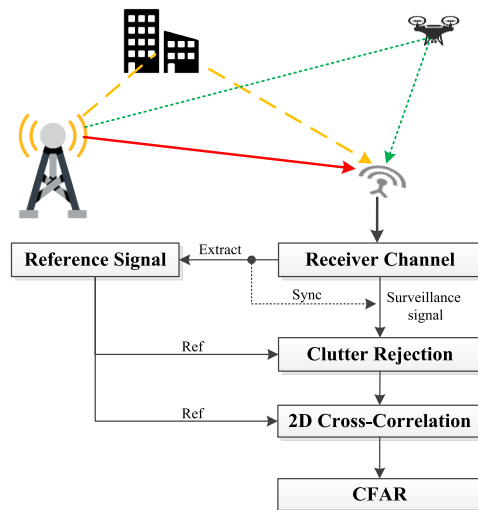


**FIGURE 1.** SDPR signal processing flow.

A description of the MSDPR for the drone detection experiments and the corresponding result analyses are shown in Section IV. Conclusions are drawn in Section V.

## II. PERFORMANCE PREDICTION

The signal processing flow for SDPR is shown in Fig. 1. First, the reference signal is extracted from the received signal after synchronization. Second, direct-path and multipath clutter are suppressed by the template of the extracted reference signal. Third, 2-D cross-correlation function between the suppressed surveillance signal and extracted reference signal is performed. Finally, the constant false alarm rate (CFAR) detection is applied to the range-Doppler (RD) map.

The receiving antenna of SDPR steers toward the surveillance area. The direct-path signal may be received by the sidelobe of the receiving antenna. The other multipath clutter is received from the mainlobe. Especially in the urban environment, the multipath clutter is even more serious, making it more difficult to extract a pure reference signal. A standard communication performance measure like bit error rate (BER) is not a sufficient metric for passive radar [21], [23]. Considering the coherent processing technology used in the SDPR signal processing, it is reasonable to adopt the correlation coefficient to assess how well the extracted reference signal matches the transmitted signal.

$$\rho = \left| \frac{E[\mathbf{s}_{ref}^H \mathbf{s}_{ref}]}{\sqrt{E[\|\mathbf{s}_{ref}\|^2]} \sqrt{E[\|\mathbf{s}_{ref}\|^2]}} \right|, \quad (1)$$

where  $\mathbf{s}_{ref}$  is the transmitted signal, and  $\mathbf{s}_{ref1}$  is the extracted reference signal from the receiver channel.

The extracted reference signal may not be completely coherent with the transmitted signal (i.e.,  $\rho < 1$ ), the multipath clutter cannot be completely suppressed. Thus, the residual multipath clutter can be expressed as [3], [23], and [24]

$$P_{rc} = (1 - \rho^2)P_c, \quad (2)$$

where  $P_c$  and  $P_{rc}$  are the power of the multipath clutter (including direct-path) before and after the multipath clutter cancellation.

Then, the 2-D cross-correlation processing is performed. The coherent integration gain  $G$  can be expressed as

$$G = \rho^2 BT, \quad (3)$$

where  $B$  is the signal bandwidth and  $T$  is the coherent integration time.

Finally, the CFAR detection method is applied. When the power of the target echo and residual multipath clutter fulfills the following inequality [25]

$$P_t G \geq (P_n + P_{rc}) T_{det}, \quad (4)$$

the target can be detected.  $P_t$  is the target echo power,  $T_{det}$  is the detection threshold, and  $P_n$  is the noise. Besides, the target echo SNR can be expressed as  $P_{TSNR} = P_t / P_n$ , and the multipath clutter to noise ratio can be expressed as  $P_{CNR} = P_c / P_n$ .

The SDPR is only equipped with a single antenna. Both the multipath and target echoes are received by this antenna. For the SDPR system, a detectable dynamic range (DDR) required to accommodate both the multipath clutter and the target echoes is given by

$$DDR = P_c / P_t = P_{CNR} / P_{TSNR}. \quad (5)$$

Substituting (2)-(4) into (5), the DDR can also be expressed as

$$\begin{aligned} DDR &= \frac{G}{T_{det}} \cdot \frac{P_{CNR}}{1 + (1 - \rho^2)P_{CNR}} \\ &= \frac{BT}{T_{det}} \cdot \frac{\rho^2 P_{CNR}}{1 + (1 - \rho^2)P_{CNR}}. \end{aligned} \quad (6)$$

The DDR of the SDPR is affected by the correlation coefficient  $\rho$  and the multipath clutter to noise ratio  $P_{CNR}$  which are coupled in practice.

To make a clear explanation between the two factors, the DDR is quantitatively analyzed. Fig. 2 shows the values of the DDR at the coherent integration gain  $BT = 67$  dB, and the detection threshold  $T_{det} = 13$  dB. The red dashed line presents the value of the DDR for the typical PR. This typical PR has two channels and one of the channels is dedicated to receive the transmitted signal. It is assumed that the transmitted signal can be completely recovered in the typical PR (i.e.,  $\rho = 1$ ).

From this picture, when the  $\rho^2$  is close 1, the DDR increases rapidly versus  $\rho^2$ . When the SDPR system station is positioned, the power of multipath clutter may be invariable. To improve the detection performance of the SDPR, an appropriate method should be used to enhance the purity of the extracted referenced signal as much as possible.

To elaborate on the detection range of the SDPR, the bistatic radar equation is used to analyze [26]. Assuming that the multipath clutter to noise ratio ( $P_{CNR}$ ) equals the

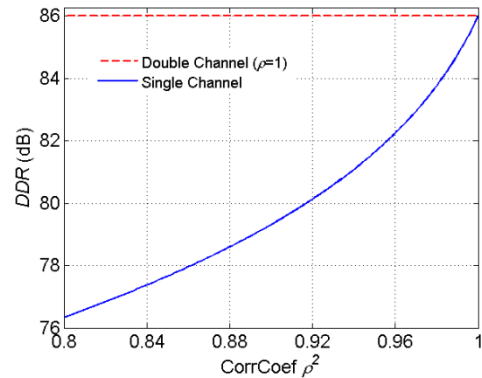


FIGURE 2. DDR versus  $\rho^2$  at  $P_{CNR} = 32$  dB ( $BT = 67$  dB,  $T_{det} = 13$  dB).

TABLE 1. Radar parameters.

Parameters	Values	Units
Center Frequency	$f_c$	MHz
Bandwidth	$B$	MHz
Bistatic RCS (DJI Phantom 4)	$\delta$	$m^2$
Integration Gain (BT)	$BT$	dB
Detection threshold	$T_{det}$	dB
Propagation loss	$(L_0 / L_1)$	1
Direct-path SNR	$P_{DNR}$	dB
Baseline Distance	$R_0$	km

Note: The RCS ( $\delta$ ) of a DJI Phantom 4 is an average value given through the HFSS 15.0 software simulation.

direct-path SNR ( $P_{DNR}$ ), the DDR of the SDPR is given as

$$DDR = \frac{P_{DNR}}{P_{TSNR}} = \left( \frac{R_1 R_2}{R_0} \right)^2 \cdot \frac{4\pi G_{R_{\theta_0}} L_1}{\sigma G_{R_{\theta_t}} L_0}, \quad (7)$$

where  $G_{R_{\theta_0}}$  is the receiver antenna's directivity gain in the direction of the transmitter,  $G_{R_{\theta_t}}$  is the receiver antenna's directivity gain in the direction of the target,  $\sigma$  is the bistatic RCS of the target,  $R_0$  is the baseline distance between the receiver (Rx) and the transmitter (Tx),  $L_0$  is the propagation loss of direct-path signal,  $R_1$  is the transmitter-to-target range,  $R_2$  is the target-to-receiver range, and  $L_1$  is the total propagation loss of the target signal from  $R_1$  to  $R_2$ .

Thus, a theoretically maximal bistatic detection area is given by the ranges  $R_1$  and  $R_2$ . Substituting (6) into (7), the detection area can be expressed as

$$\left( \frac{R_1 R_2}{R_0} \right)^2 = \frac{\sigma G_{R_{\theta_t}} L_1}{4\pi G_{R_{\theta_0}} L_0} \cdot \frac{BT}{T_{det}} \cdot \frac{\rho^2 P_{DNR}}{1 + (1 - \rho^2)P_{DNR}}, \quad (8)$$

where  $BT$ ,  $T_{det}$ ,  $\sigma$ ,  $L_0$ ,  $L_1$  is determined by the model of the SDPR system. From (8), the detection area of the SDPR is determined by the receiver antenna's directivity gain, the correlation coefficient  $\rho$ , and the direct-path signal to noise ratio  $P_{DNR}$ .

Table 1 gives the parameters based on the following experimental scenes. The receiving antenna is a yagi antenna with a gain of 10 dB. The H-plane pattern is shown in Fig. 3. The angle between the antenna boresight and the transmitter

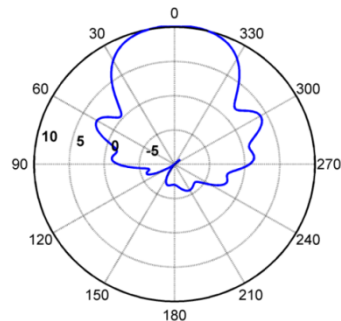


**FIGURE 3.** H-plane pattern of yagi antenna.

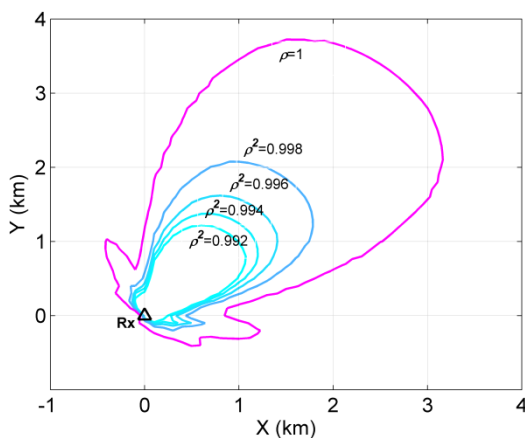


**FIGURE 4.** Contours of detection range for SDPR (Rx represents receiver station,  $P_{DNR} = 32$  dB).

is  $130^\circ$ . The estimation result is shown in Fig. 4, where the  $P_{DNR} = 32$  dB, the different detection ranges are given with  $\rho^2 = 0.992, 0.994, 0.996, 0.998$ , and 1, respectively. It is clearly indicated that the purity of the reference signal has a significant influence on the detection range of the SDPR. To improve the detection range, an appropriate method is used to refine the reference signal, which will be discussed in following section.

### III. SIGNAL PROCESSING METHOD

The feasibility of SDPR for the drone detection has been analyzed from the systematic level theoretically. Since the SDPR is equipped with only a single receiver channel, the design and application of such radar face great challenges. These challenges originate from the extensive multipath clutter interference caused by the complex urban propagation environment and the detection of the target with a small RCS and slow speed (such as UAV). Thus, key signal processing methods including reference signal extraction and multistatic signal processing are analyzed.

#### A. SIGNAL MODEL

In the ultrahigh frequency (UHF) band, it is reasonable approach to model the ground clutter and multipath clutter as a set of stationary point scatterers. Based on this

assumption, the complex envelope of the total signal in the receiver channel is given by

$$s(t) = [A_0 d(t) + \sum_{n=1}^{N_c} A_n d(t - \tau_n) + \sum_{m=1}^{N_t} B_m d(t - \tau_m) e^{j2\pi f_{dm} t}] \\ \times e^{j2\pi f_{cd} t} + n(t), \quad (9)$$

where  $d(t)$  is the complex envelope of the direct-path signal (a delayed replica of the transmitted signal);  $A_0$  is the complex amplitude of the direct-path signal received via the side/backlobe of the receiving antenna;  $A_n$  and  $\tau_n$  are the complex amplitude and the delay (with respect to the direct-path signal) of the  $n$ th stationary scatter ( $n = 1, \dots, N_c$ );  $B_m$ ,  $\tau_m$  and  $f_{dm}$  are the complex amplitude, the delay (with respect to the direct-path signal) and the Doppler frequency of the  $m$ th target ( $m = 1, \dots, N_t$ );  $f_{cd}$  is the carrier frequency offset (CFO) between the transmitter and the receiver;  $n(t)$  is the thermal noise contribution at the receiver channel.

In the SDPR system, the receiving antenna steers toward the surveillance area as shown in Fig. 1. Since the multipath clutter may be received by the mainlobe of the receiving antenna, especially in the urban environment, the amplitude of the direct-path signal ( $A_0$ ) is not necessarily greater than the strongest amplitude ( $A_i = \max\{A_1, \dots, A_{N_c}\}$ ) of the multipath clutter. Moreover, it is possible that the direct-path signal is even blocked by tall buildings ( $A_0 = 0$ ).

When the strongest path signal is not the direct-path signal ( $A_0 < A_i$  or  $A_0 = 0$ ), the time synchronization may not exactly estimate the starting position of an OFDM symbol (i.e., unable to accurately estimate the time-of-arrival (TOA) of the direct-path signal), which will affect bistatic range estimation. It is not trivial to locate and track the detected target by multiple bistatic ranges in the MSDPR system. This problem will be studied in Section III-C.

Although the TOA of the direct-path signal may not be accurately estimated, using the strongest path signal is still effective for the CFO estimation and reference signal extraction due to the excellent signal structure of the digital television broadcasting signal.

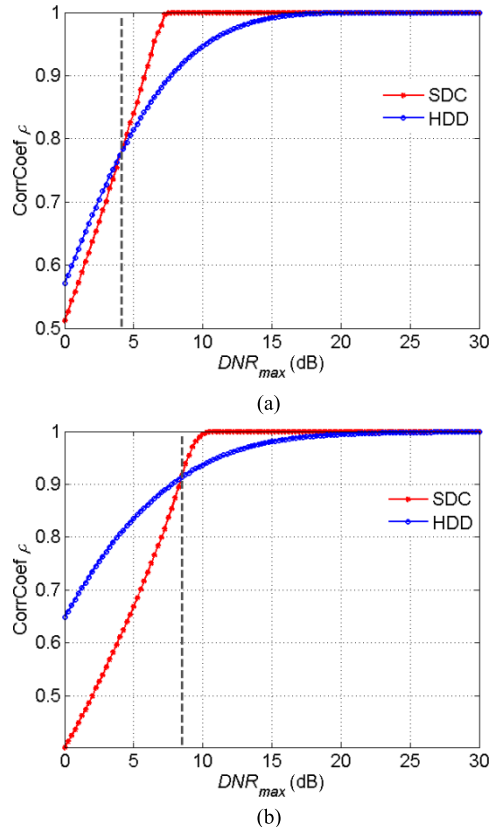
#### B. REFERENCE SIGNAL EXTRACTION

The reference signal extraction is a significant part of the SDPR signal processing. For digital television broadcasting signal, an effective approach is to reconstruct reference signal by taking advantage of the OFDM signal's features, which is robust to noise and multipath clutter interferences. It is especially important when the “reference antenna” steers towards the monitoring area rather than the transmitter. The reference signal reconstruction consists of four procedures, namely synchronization, channel equalization, soft decoding plus forward error correction (SDC) or hard-decision decoding (HDD), and remodulation. The HDD decodes each datum directly to the closest constellation point, which needs less information about the transmitted signal.

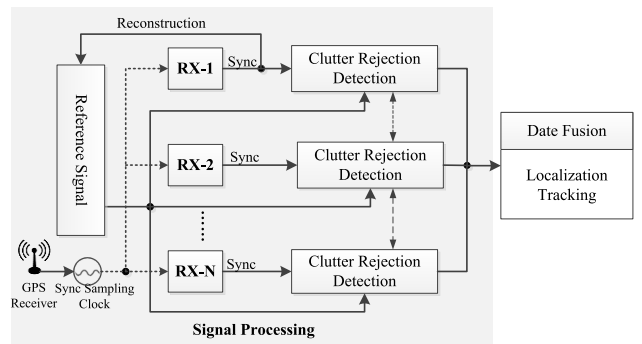
Except for solving the key problems (i.e., time synchronization, CFO and sampling rate offset estimation and

**TABLE 2.** The profile of COST207 typical urban (TU) channel.

	Tap1	Tap2	Tap3	Tap4	Tap5	Tap6	Unit
Delay	0	0.2	0.5	1.6	2.3	5	$\mu\text{s}$
Power	-3	0	-5	-6	-8	-10	dB

**FIGURE 5.** Correlation coefficient  $\rho$  performance under TU channel.  
(a) 4-QAM. (b) 16-QAM.

compensation), we should choose a reasonable method from the SDC and the HDD after the channel equalization to recover the transmitted signal as much as possible. In general, the reference signal reconstruction through SDC method can obtain a clean transmitted signal. However, when the SINR of the direct-path (or the strongest path) is relatively low, utilizing the SDC method may be not appropriate, as the equalized signal is beyond the ability of the decoding and forward error correction. In addition, when the direct-path SINR is relatively high, there is no need to recover the transmitted signal with the tedious forward error correction, as the transmitted signal can be obtained by the simple HDD method efficiently. To illustrate this problem, a simulation is conducted. The main parameters involved in the simulation are listed in Table 2. 500 independent simulations are performed against each  $DNR_{max}$  value, where the  $DNR_{max}$  is the strongest path SNR. The simulation results are shown in Fig. 5. 5.

**FIGURE 6.** MSDPR processing flow diagram.

As analyzed in Section II, the correlation coefficient  $\rho$  is used to evaluate which method is better to reconstruct the transmitted signal. From Fig. 5(a), when  $DNR_{max} < 4$  dB, the reconstructed signal by HDD method has a closer correlation with the transmitted signal. Meanwhile, when  $DNR_{max} > 20$  dB, the HDD method can excellently reconstruct the transmitted signal. Hence, under this simulation condition, when  $DNR_{max} < 4$  dB or  $DNR_{max} > 20$  dB, the simple HDD method is chosen. Similarly, in Fig. 5(b), when  $DNR_{max} < 8.5$  dB or  $DNR_{max} > 28$  dB, the HDD method is reasonable to reconstruct the transmitted signal.

### C. MSDPR PROCESSING METHOD

It is impossible to locate and track target using a single SDPR because the SDPR can only detect target's bistatic range and bistatic velocity. To solve this problem, three distributed SDPR stations are needed at least [27]. Combining with the signal structure of the digital television broadcasting signal, an MSDPR processing method is proposed. Differing from the conventional signal processing method that each receiving station processes separately, including reference signal extraction and clutter rejection, this method utilizes the optimal reference signal restructured from the receiving station with the least interference as the shared reference signal for all the receiving stations. Fig. 6 depicts this processing flow diagram. Through the propagation channel analysis, the receiving station with the least multipath interference is selected to extract the optimum reference signal. Meanwhile, appropriate clutter rejection method is chosen for each receiving station. After CFAR detection, the data of each Tx-Rx (bistatic) pair is uploaded to the data fusion center. In the data fusion center, data association, elliptical localization technique and Kalman filter are applied. If a real-time processing is demanded, there is a requirement that the multistatic signal needs to be transmitted to the signal fusion center in real time. This requirement will be considered in our future work.

The advantages of this processing approach are mainly reflected in following three aspects.

- 1) Optimum reference signal among multistation can be obtained. It is used as multipath clutter rejection and cross-correlation processing by all stations.

2) System detection performance, adaptability and robustness can be improved. As the reference signal is extracted from one of receiving stations, the other receiving stations have no need to weigh direct-path SINR and target SNR. Multipath clutter cancellation of the MSDPR is more effective by the optimum extracted reference.

3) Computational burden can be reduced.

To accurately achieve the target locating and tracking, two key problems of the MSDPR need to be solved.

1) Multipath clutter cancellation. Multipath clutter is suppressed by the template of the extracted reference signal with the theory of adaptive coherent subtraction. The performances of the multipath clutter rejection methods based on this theory are affected by the non-ideal factors such as non-zeros Doppler multipath clutter, fractional time delay of multipath clutter, CFO, sampling rate offset and so on [13], [23], [24], [29]. The methods presented in [28]–[31] take advantages of the OFDM modulation with a cyclic prefix (CP). In [29], the method ECA-CD which has the robustness to the fractional time delay of multipath clutter and the sampling rate offset, mainly considers the non-zeros Doppler multipath clutter rejection. The non-zeros Doppler multipath clutter in the “surveillance channel” may be caused by the inaccurate CFO compensation. However, when the delays of multipath clutter exceed the CP of the OFDM symbol (in this case, we name the multipath clutter as far clutter), the multipath clutter cannot be completely suppressed by the ECA-CD. The reason is that the far clutter cause inter-symbol interference (ISI) and damage the orthogonality of the subcarriers in the OFDM symbol [6], [31]. A method in [24] is chosen in this situation. The generalized subband cancellation method therein is carried out in time domain and also considers these non-ideal factors.

Hence, the two methods of the clutter rejection are chosen separately in different multipath clutter interference environments. When the multipath clutter includes the strong far clutter, the time domain method presented in [24] is chosen. In general, the frequency domain method ECA-CD presented in [29] is used to suppress the multipath clutter.

2) The data of each Tx-Rx bistatic range for the target needs to be estimated accurately. MSDPR adopts time difference of arrival (TDOA) location technique. It is necessary to accurately measure the bistatic range of the detected target in each SDPR. Analyzed in Section III-A, the key problem is equivalent to accurately estimate the TOA of the direct-path signal in each SDPR. Hence, the following two methods are used.

One is the empirical threshold value method. In general, compared with multipath signals, the direct-path signal is not necessarily the strongest path, but it is the first arrival. When the SDPR receives the direct-path signal, we can estimate the TOA of the direct-path signal with the empirical threshold value method, which is simply and easily implemented [32].

Another one is the calibration method, utilizing the known target position information to compensate the fixed offset. When the direct-path signal is blocked, or the direct-path

signal is interfered by the dense and strong multipath clutter, or the sampling clock jitters in the MSDPR, the empirical threshold value method may not accurately seize the position of arrival of the direct-path signal. In this case, the empirical threshold value method is used to ensure that the starting point of the “surveillance channel” after each synchronous processing is in the same position where there is a fixed offset from the position of arrival of the direct-path signal. And then the calibration method is used to compensate the fixed offset. In practice, the two methods are usually used together to ensure the accurate estimation of the bistatic range.

## IV. FIELD EXPERIMENTS AND RESULTS

### A. EXPERIMENTAL SCENARIO

Fig. 7 depicts the scenario of the drone detection experiment where the MSDPR system has a multistatic configuration with one transmitter and three receivers. The transmitter is the Guishan tower. The three receivers, marked as Receiver A, B, and C, are deployed in Wuhan University, Wuhan, China. It should be noted that the receiving antenna height (about 12m) of Receiver C is lower than the other two receivers (about 20m). The baselines between the transmitter and receivers are from 7.6km to 8.2km, respectively. The receiving antennas used in three receivers are UHF-band Yagi antennas with 10 dB nominal gain. The H-plane pattern is shown in Fig. 3. As a cooperative target, a quadcopter (DJI Phantom 4) is used for experimental trial. The flight records of this quadcopter can provide ground truth for the evaluation. For comparison, three reference antennas steering toward the transmitter are also arranged at the three stations, respectively. The reference antennas are the same type of UHF-band Yagi antennas.

The MSDPR system has a central controller to control the coordinated work via an internetwork. The sampling clocks of the three receivers are based on GPS clock. Through mixing, amplifying, and filtering in the analog front end, the signal is digitalized by the Analog to Digital Converter (ADC). After digital down conversion, the data are uploaded to the computer server for the data storage and offline analysis.

A series of drone detection experiments on MSDPR were systematically conducted by Wuhan University under the above mentioned scenario in July 2017. The experimental results of SDPR and MSDPR are introduced in detail in the following subsections.

### B. EXPERIMENTAL RESULTS

To illustrate multipath propagation environment of the three stations in the surveillance area, the results of channel estimation are shown in Fig. 8(a). Compared with the other two stations, Receiver C presents the most serious multipath clutter interference. Some of clutter even exceeds the CP of the OFDM symbol. In contrast, Receiver A has the least multipath clutter interference. In Receiver C, The results of channel estimation between the surveillance channel and reference channel are presented in Fig. 8(b), where there exists a



**FIGURE 7.** Scenario of drone detection experiment trial.

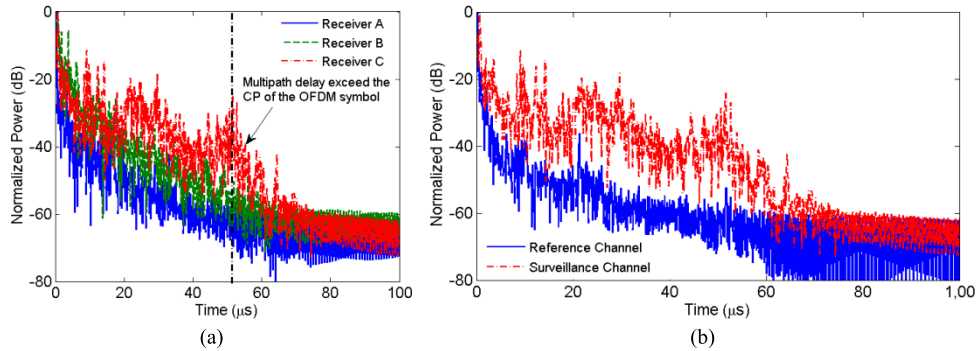


**FIGURE 8.** (a) Multipath propagation in the surveillance area (Receiver A, Receiver B, and Receiver C). (b) Multipath propagation in Receiver C (Reference and surveillance channels).

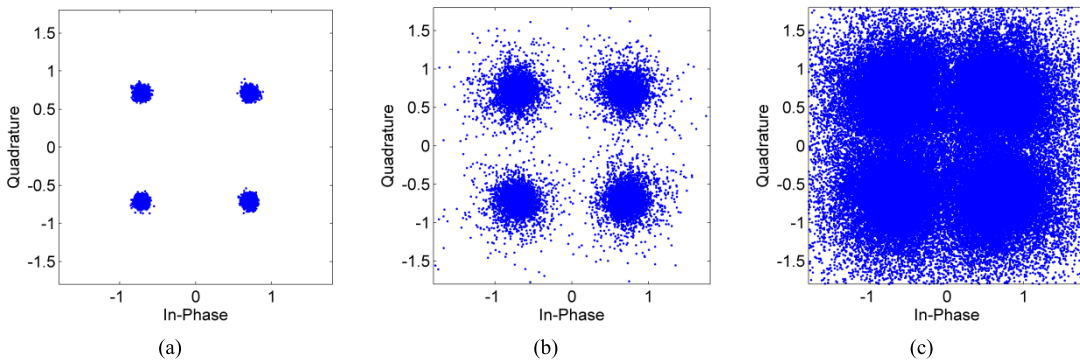


**FIGURE 9.** Constellation diagram. (a) Receiver A. (b) Receiver B. (c) Receiver C.

0.5  $\mu$ s delay between the peak positions of the two channels. It can also be found that Receiver A and Receiver B have a 0.2  $\mu$ s and 0.3  $\mu$ s delay respectively. It demonstrates that the strongest multipath signal is not the direct-path signal in this experimental scenario. From Fig. 8(a) and Fig. 8(b), the following two points can be figured out: 1) the frequency

domain method (ECA-CD) is not suitable for the multipath clutter cancellation in Receiver C. 2) In MSDPR, Receiver A is used to reconstruct the reference signal.

The obtained constellation diagrams of the three Receivers at the same time after synchronization and channel equalization are shown in Fig. 9. For Receiver A, the HDD method

can be used to reconstruct the reference signal because the strongest path signal SNR can be roughly estimated more than 25 dB in Fig. 8(a). It's not necessary to use the relatively complicated SDC method. While with respect to Receiver B and Receiver C, the SDC method is used to reconstruct the reference signal than HDD. Hence, it is indicated that the reference signal extraction method needs to be reasonably chosen according to the surveillance area's multipath propagation environment.

To illustrate the influence of the reconstructed reference signal purity on the detection performance of the SDPR, we analyze the data of Receiver C, whose duration is about 3 minutes. The clutter rejection ratio (CR) is defined as  $CR = P_c/P_{rc}$ . As the transmitted signal is unknown, the reconstructed reference signal from the reference antenna is regarded as a clean and benchmark signal for comparison. The correlation coefficient  $\rho$  is the correlation strength between the benchmark reference signal and the SDPR's reconstructed reference signal. The CR difference between the benchmark reference signal and the reconstructed reference signal is named clutter rejection ratio loss  $CR\_Loss$ , namely,

$$CR\_Loss = CR_1/CR_0, \quad (10)$$

where  $CR_1$  is the result of utilizing the reconstructed reference signal, and  $CR_0$  is the result of utilizing the benchmark reference signal. Fig. 10(a) shows the corresponding relationship between  $\rho$  and  $CR\_Loss$ , which is able to clearly indicate that the smaller  $\rho$  is, the higher the value of  $CR\_Loss$  is.

The results after CFAR detection are described in Fig. 10(b) and Fig. 10(c). Specifically, Fig. 10(b) is the detection result with two channels (reference and surveillance channels), and Fig. 10(c) is the detection result with the single channel (surveillance channel used as reference and surveillance channel). The clutter rejection method and the parameters of CFAR are all the same. Comparing the two pictures, the target SNR in Fig. 10(c) is generally about 5 dB lower than that in Fig. 10(b). Meanwhile, more weak targets and false alarms are presented in Fig. 10(b). In general, the pure reference signal will enhance the performance of clutter rejection, which is beneficial to the weak target detection. Hence, for the SDPR, when the power of received multipath clutter is invariable, to improve the detection performance, we should recover the reference signal as much as possible.

### C. LOCATING AND TRACKING

At last, to achieve the UAV locating and tracking, the three stations are used for joint detection. A maneuvering trajectory including uniform linear motion and turning is shown in Fig. 12(a). Fig. 11 presents the potential target detections of each receiver after CFAR detection and the GPS records of the flight. Although there are some false alarms, the agreement between the grey experimental results and the red ground truth result is clearly visible. It validates the successful detection of drone using the SDPR. The tracking result and the GPS records of the drone in this experiment are

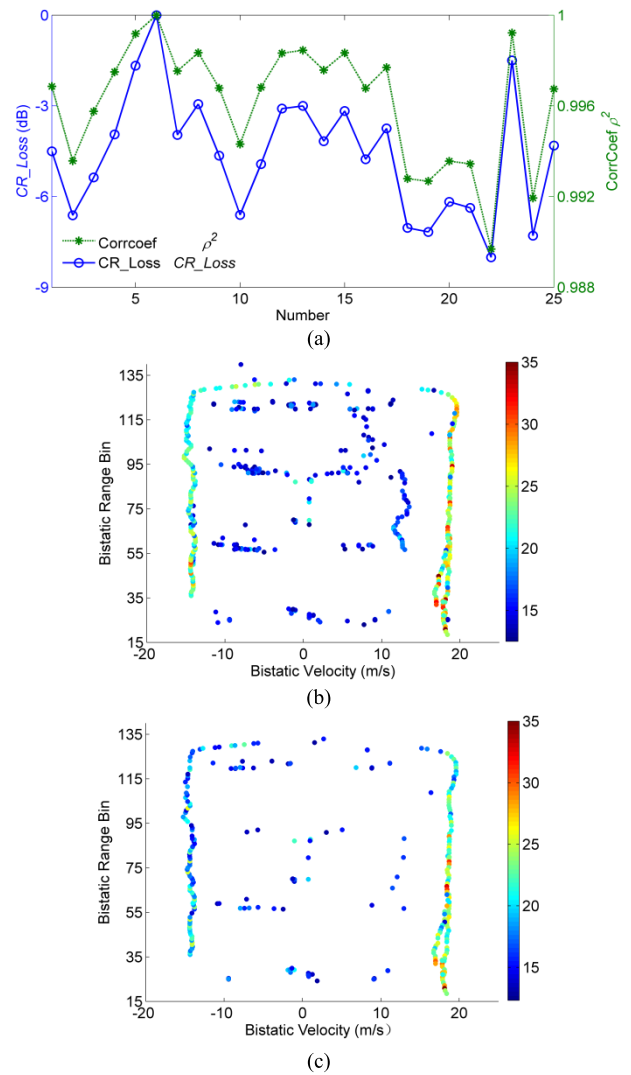


**FIGURE 10.** (a) The corresponding relationship between  $\rho$  and  $CR\_Loss$ . (b) Detection results over RD map with two receiving channels (Ref. and Surv. channels) in Receiver C. (c) Detection results over RD map with the single channel (Surv. channel) in Receiver C.

presented in Fig. 12(b) where the tracking trajectory almost coincides with the ground truth. MSDPR adopts TDOA location technique. It utilizes multiple bistatic ranges to get more accurate target position, which is different from the previous bistatic system combining azimuth and bistatic range to locate target. Note that the trajectory is not continuous during the turning because it enters the clutter region of the three receivers almost simultaneously when the drone turns. As a result, network optimization is a key technology with regard to the MSDPR system. In summary, the feasibility and validity of using the MSDPR for Drone Detection is verified.

### V. CONCLUSIONS AND FUTURE WORK

The paper presents the signal processing method and experimental results of the SDPR and MSDPR for the drone detection. It is an interesting trial on this component version of the passive radar. The theoretical analysis of the SDPR detection

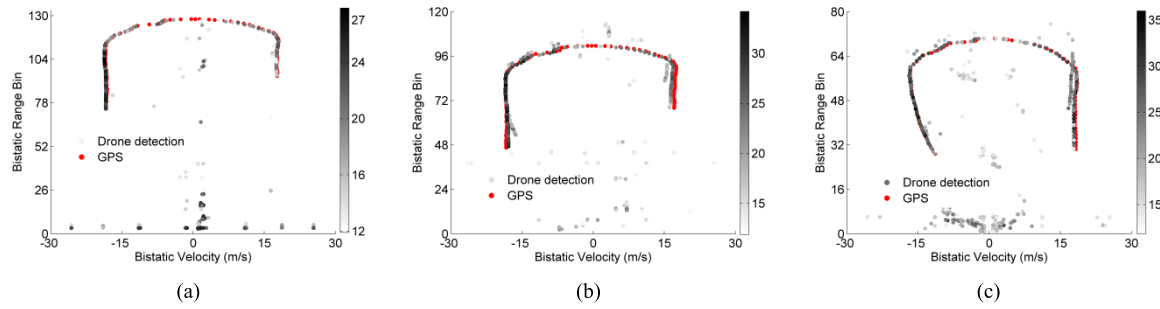


**FIGURE 11.** Detection results over the RD map. (a) Receiver A. (b) Receiver B. (c) Receiver C.

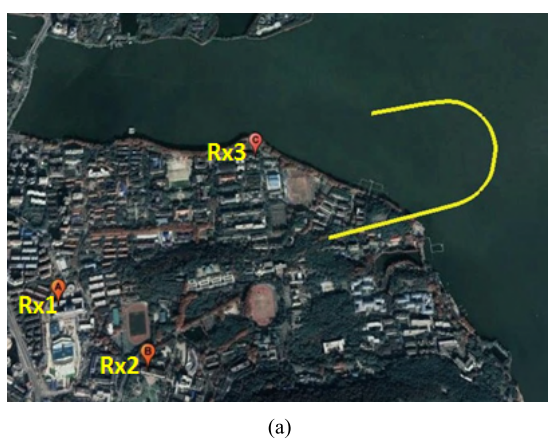


**FIGURE 12.** (a) Target trajectory of DJI Phantom 4 in MSDPR. (b) Track result compares with GPS.

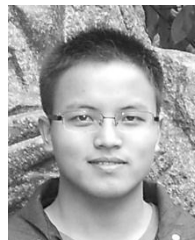
range is reported. According to the characteristics of digital broadcast signals, the reference signal extraction is analyzed and a novel MSDPR processing method is proposed. The core idea of this method is to use the optimal reference signal extracted from the receiving station with the least interference as the shared reference signal, which can greatly improve the system detection capability.

Be that as it may, several aspects need to be further studied. The SDPR detection performance and multipath clutter rejection needs to be researched in different experimental environments. More attention should be paid to the application for low-altitude target detection, classification and recognition (such as UAVs and birds). In addition, the distributed SDPR network optimization to improve detection performance will also be a key topic.

## REFERENCES

- [1] M. Ritchie, F. Fioranelli, and H. Borrión, "Micro UAV crime prevention: Can we help Princess Leia?" in *Preventing Crime in the 21st Century*, B. L. Savona and Ed. Cham, Switzerland: Springer, 2017, pp. 359–376.
- [2] J. E. Palmer, H. A. Harms, S. J. Searle, and L. Davis, "DVB-T passive radar signal processing," *IEEE Trans. Signal Process.*, vol. 61, no. 8, pp. 2116–2126, Apr. 2013.
- [3] X. Wan, J. Yi, Z. Zhao, and H. Ke, "Experimental research for CMMB-based passive radar under a multipath environment," *IEEE Trans. Aerosp. Electron. Syst.*, vol. 50, no. 1, pp. 70–85, Jan. 2014.
- [4] R. Tao, Z. Gao, and Y. Wang, "Side peaks interference suppression in DVB-T based passive radar," *IEEE Trans. Aerosp. Electron. Syst.*, vol. 48, no. 4, pp. 3610–3619, Oct. 2012.
- [5] R. Tao, H. Wu, and T. Shan, "Direct-path suppression by spatial filtering in digital television terrestrial broadcasting-based passive radar," *IET Radar, Sonar Navigat.*, vol. 4, no. 6, pp. 791–805, Dec. 2010.
- [6] L. Fang, X. Wan, G. Fang, F. Cheng, and H. Ke, "Passive detection using orthogonal frequency division multiplex signals of opportunity without multipath clutter cancellation," *IET Radar, Sonar Navigat.*, vol. 10, no. 3, pp. 516–524, 2016.
- [7] D. Poulline, "UAV detection and localization using passive DVB-T radar MFN and SFN," 2016. [Online]. Available: <https://www.semanticscholar.org/>
- [8] Y. Liu, X. Wan, H. Tang, J. Yi, Y. Cheng, and X. Zhang, "Digital television based passive bistatic radar system for drone detection," in *Proc. IEEE Radar Conf.*, Seattle, WA, USA, May 2017, pp. 1493–1497.
- [9] H. D. Griffiths, "From a different perspective: principles, practice and potential of bistatic radar," in *Proc. Int. Radar Conf.*, Adelaide, SA, Australia, Sep. 2003, pp. 1–7.
- [10] H. Kuschel and D. O'Hagan, "Passive radar from history to future," in *Proc. 11th Int. IRS*, Vilnius, Lithuania, 2010, pp. 1–4.
- [11] J. Palmer, S. Palumbo, A. Summers, D. Merrett, S. Searle, and S. Howard, "An overview of an illuminator of opportunity passive radar research project and its signal processing research directions," *Digit. Signal Process.*, vol. 21, no. 5, pp. 593–599, Sep. 2011.
- [12] J. Liu, H. Li, and B. Himed, "On the performance of the cross-correlation detector for passive radar applications," *Signal Process.*, vol. 113, pp. 32–37, Aug. 2015.
- [13] F. Colone, D. W. O'Hagan, P. Lombardo, and C. J. Baker, "A multistage processing algorithm for disturbance removal and target detection in passive bistatic radar," *IEEE Trans. Aerosp. Electron. Syst.*, vol. 45, no. 2, pp. 698–722, Apr. 2009.
- [14] S. Searle, S. Howard, and J. Palmer, "Remodulation of DVB-T signals for use in passive bistatic radar," in *Proc. Asilomar Conf. Signals Syst. Comput. (ASILOMAR)*, Pacific Grove, CA, USA, 2010, pp. 1112–1116.

- [15] H. Kuschel, M. Ummenhofer, D. O'Hagan, and J. Heckenbach, "On the resolution performance of passive radar using DVB-T illuminations," in *Proc. 11th Int. IRS*, Vilnius, Lithuania, 2010, pp. 20–23.
- [16] M. K. Baczyk and M. Malanowski, "Reconstruction of reference signal in DVB-T-based passive radar," *Int. J. Eletron. Telecommun.*, vol. 57, no. 1, pp. 43–48, Mar. 2011.
- [17] W. Xianrong, W. Junfang, H. Sheng, and T. Hui, "Reconstruction of reference signal for DTMB-based passive radar systems," in *Proc. IEEE CIE Int. Conf. Radar*, Chengdu, China, Oct. 2011, pp. 165–168.
- [18] X. Wan, B. Cen, J. Yi, L. Fang, and H.-Y. Ke, "Reference signal extraction methods for CMMB-based passive bistatic radar," *J. Electron. Inf. Technol.*, vol. 34, no. 2, pp. 338–343, Feb. 2012.
- [19] W. C. Barott and J. Engle, "Single-antenna ATSC passive radar observations with remodulation and keystone formatting," in *Proc. IEEE Radar Conf.*, Cincinnati, OH, USA, May 2014, pp. 0159–0163.
- [20] M. K. Baczyk, K. Kulpa, P. Samczynski, and M. Malanowski, "The impact of reference channel SNR on targets detection by passive radars using DVB-T signals," in *Proc. IEEE Radar Conf.*, Arlington, VA, USA, May 2015, pp. 708–712.
- [21] S. Searle, L. Davis, and J. Palmer, "Signal processing considerations for passive radar with a single receiver," in *Proc. IEEE Conf. ICASSP*, Brisbane, QLD, Australia, Apr. 2015, pp. 5560–5564.
- [22] O. Mahfoudia, F. Horlin, and X. Neyt, "On the feasibility of DVB-T based passive radar with a single receiver channel," in *Proc. Int. Conf. Radar Syst.*, Oct. 2017, pp. 1–6.
- [23] Z. H. Zhou, T. Shan, Y. Feng, S. H. Liu, and J. Zhang, "A subbandadaptive filter for DTV based passive radar," in *Proc. IET Int. Radar Conf.*, Xi'an, China, 2013, pp. 534–537.
- [24] J. Yi, X. Wan, D. Li, and H. Leung, "Robust clutter rejection in passive radar via generalized subband cancellation," *IEEE Trans. Aerosp. Electron. Syst.*, to be published, doi: [10.1109/TAES.2018.2805228](https://doi.org/10.1109/TAES.2018.2805228).
- [25] H. A. Harms, J. E. Palmer, S. J. Searle, and L. M. Davis, "Impact of quantization on passive radar target detection," in *Proc. IET Int. Conf. Radar Syst.*, Glasgow, U.K., Oct. 2012, pp. 1–6.
- [26] M. Malanowski, K. Kulpa, J. Kulpa, P. Samczynski, and J. Misiurewicz, "Analysis of detection range of FM-based passive radar," *IET Radar, Sonar Navigat.*, vol. 8, no. 2, pp. 153–159, Feb. 2014.
- [27] M. Malanowski and K. Kulpa, "Two methods for target localization in multistatic passive radar," *IEEE Trans. Aerosp. Electron. Syst.*, vol. 48, no. 1, pp. 572–580, Jan. 2012.
- [28] Z. Zhao, X. Wan, Q. Shao, Z. Gong, and F. Cheng, "Multipath clutter rejection for digital radio mondiale-based HF passive bistatic radar with OFDM waveform," *IET Radar, Sonar Navigat.*, vol. 6, no. 9, pp. 867–872, Dec. 2012.
- [29] C. Schwark and D. Cristallini, "Advanced multipath clutter cancellation in OFDM-based passive radar systems," in *Proc. IEEE Radar Conf.*, Philadelphia, PA, USA, May 2016, pp. 1–4.
- [30] Z. Zhao, X. Zhou, S. Zhu, and S. Hong, "Reduced complexity multipath clutter rejection approach for DRM-based HF passive bistatic radar," *IEEE Access*, vol. 5, pp. 20228–20234, Sep. 2017.
- [31] J.-X. Yi, X.-R. Wan, Z.-X. Zhao, F. Chen, and H.-Y. Ke, "Subcarrier-based processing for clutter rejection in CP-OFDM signal-based passive radar using SFN configuration," *J. Radars*, vol. 2, no. 1, pp. 1–13, Jan. 2013.
- [32] D. Dardari, C.-C. Chong, and M. Z. Win, "Threshold-based time-of-arrival estimators in UWB dense multipath channels," *IEEE Trans. Commun.*, vol. 56, no. 8, pp. 1366–1378, Aug. 2008.



**JIANXIN YI** was born in Hunan, China, in 1989. He received the B.E. degree in electrical and electronic engineering and the Ph.D. degree in radio physics from Wuhan University, China, in 2011 and 2016, respectively. From 2014 to 2015, he was a Visiting Ph.D. Student with the University of Calgary, Canada. He currently holds a post-doctoral position at the School of Electronic Information, Wuhan University. His main research interests include radar signal processing, target tracking, and information fusion.



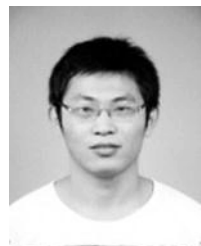
**XIANRONG WAN** was born in Hubei, China, in 1975. He received the B.E. degree from the Wuhan Technical University of Surveying and Mapping, China, in 1997, and the Ph.D. degree from Wuhan University, China, in 2005. He is currently a Professor and a Ph.D. Candidate Supervisor with Wuhan University. Recent years, he has hosted and participated in over 10 national research projects, and published over 70 academic papers. His main research interests include design of new radar system such as passive radar, over-the-horizon radar, and array signal processing.



**YUQI LIU** was born in Hubei, China, in 1990. He received the B.E. degree from Wuhan University, China, in 2013, where he is currently pursuing the Ph.D. degree with the School of Electronic Information. His main area of interest is in signal processing of passive radar and array signal processing.



**HENGYU KE** was born in Hubei, China, in 1957. He received the Ph.D. degree from Wuhan University in 1996. He is currently a Professor and a Ph.D. Candidate Supervisor with Wuhan University. His main research interests include electromagnetic radiation and scattering, high-frequency radar ocean remote sensing, radio propagation, and antenna.



**GAO FANG** was born in Hubei, China, in 1989. He received the B.E. degree from the Wuhan Institute of Technology, China, in 2012. He is currently pursuing the Ph.D. degree with the School of Electronic Information, Wuhan University. His main research interests include passive radar system design and signal processing of passive radar.